Ballistic Conductance Fluctuations in Shape Space

I. H. Chan, R. M. Clarke, and C. M. Marcus
Department of Physics, Stanford University, Stanford, California 94305-4060

K. Campman and A. C. Gossard
Materials Department, University of California at Santa Barbara, Santa Barbara, California 93106
(Received 12 August 1994)

Ballistic conductance fluctuations were measured in a GaAs quantum dot as a function of shape distortion and magnetic field. Shape distortion provides a novel source of conductance fluctuations and creates an effective "ensemble of dots," allowing statistics to be studied at fixed field. Continuous changes in fluctuation statistics due to breaking of time-reversal symmetry are seen about zero magnetic field. Throughout, conductance fluctuation distributions appear Gaussian. The power spectrum of shape fluctuations appears exponential over three decades.

PACS numbers: 72.20.My, 05.45.+b, 73.20.Fz

Our understanding of how classical chaos arises from quantum mechanics has been extended recently by experiments and theory connecting quantum chaos and mesoscopic physics [1–8]. Of particular interest recently [5,6,9–16] are random conductance fluctuations in quantum dots—small conductors comparable in size to the phase-coherence length ℓ_φ of the electrons traveling through them. Interference effects from coherent electrons cause random but repeatable fluctuations in the conductance as parameters such as magnetic field [2,5,16], Fermi energy [6,13], or shape [17] are changed. A variety of theoretical approaches [2,10–12,18] have been used to investigate aspects of these conductance fluctuations, leading to a rather detailed understanding of their origin and character.

With improvements in semiconductor material quality and submicron fabrication technology, it has become possible to fabricate quantum dots in which not only ℓ_φ but also the elastic mean free path ℓ exceeds the device dimensions. This new regime of ballistic transport has opened up greater experimental horizons to the study of quantum chaos and mesoscopic physics, and in the last few years a number of experiments investigating ballistic conductance fluctuations as a function of magnetic field [5,16,19] and Fermi energy [6] have appeared.

In this Letter, we expand the list of experimental parameters that induce ballistic conductance fluctuations to include shape distortion. Shape-induced fluctuations in mesoscopics are of considerable theoretical interest in their own right [17] and have not been previously reported experimentally. Moreover, for dots in which electron trajectories are chaotic, shape distortion effectively creates an "ensemble of dots." Such an effective ensemble allows universal statistical features of conductance fluctuations to be extracted while dot-specific features tend to average away [9]. It also allows the distribution of conductances at a fixed parameter such as magnetic field to be measured.

An electron micrograph of the quantum dot we measured is shown in Fig. 1(b). The structure was formed using standard gate depletion of a two-dimensional electron gas (2DEG) in a GaAs/AlGaAs heterostructure, with the 2DEG 800 Å beneath the surface. Gates were patterned using electron beam lithography to define a square shape $\sim$1.7 μm on a side with $\sim$250 nm wide point contacts in adjacent corners. Assuming a depletion width of $\sim$80 nm gives a dot area A of $\sim$2.4 μm^2. The conductance of the two point-contact leads were independently

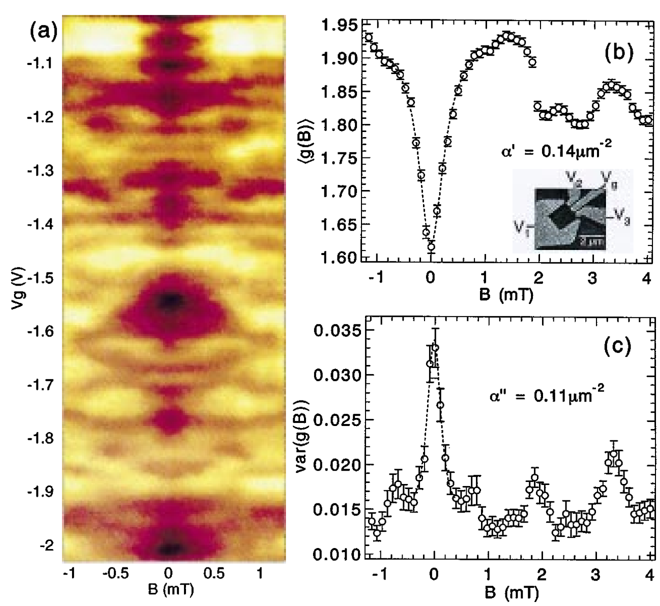

FIG. 1. (a) Color map of conductance fluctuations $\delta g(V_g, B)$ (in units of e^2/h) as a function of magnetic field B and gate voltage V_g, which controls shape distortion. Note the symmetry about $B = 0$. (b) Shape-averaged conductance $\langle g(B) \rangle$ shows a minimum at $B = 0$ due to weak localization. Dashed curve is fit to Eq. (1). Inset: electron micrograph of device. V_g is used to produce shape distortion. (c) Variance var$[g(B)]$ of shape-distortion conductance fluctuations [in units of $(e^2/h)^2$] shows a peak at $B = 0$. Dashed curve is fit by Eq. (2).

 0031-9007/95/74(19)/3876(4)$06.00

adjusted by setting V_2 and V_3 [see inset of Fig. 1(b)], so that each had a conductance $g = 4$ in units of e^2/h (i.e., each lead passed ~ 2 spin-degenerate modes), giving an average conductance through the dot of $\sim 2e^2/h$ (fully randomized trajectories yield Ohmic addition of average resistances [20]). The gate voltage V_g was used to slightly change the shape of the dot. Assuming a depletion width proportional to gate voltage [21], shape distortion has a small effect (<5%) on the total dot area over the range of gate voltage investigated ($-2 < V_g < -1$ V). A 2DEG mobility of 1×10^6 cm^2/V s and sheet density of 3.5×10^{11} cm^{-2} were measured after fabrication with all gates floating. This yields a transport mean free path ℓ of ~ 9 μm, considerably larger than the size of the dot. We do not expect our results to depend on ℓ being much greater than the dot dimensions, only that transport not be strongly diffusive within the dot.

The resistance of the dot was measured in a dilution refrigerator at base temperature ($T_{\mathrm{fridge}} \sim 30$ mK) using a 0.1 nA current bias and standard four-wire lock-in techniques at 17.5 Hz. With the other gates held fixed at ~ -1 V, the shape-distorting gate voltage V_g was swept between –2 and –1 V. A perpendicular magnetic field B was incremented by 0.1 mT following each voltage sweep, producing a raster scan of the conductance landscape in the shape–B-field plane. A smooth background conductance showing a $\sim 30\%$ variation along the V_g direction but essentially flat along the B direction was subsequently subtracted from the raw data to give the conductance fluctuation $\delta g(V_g, B)$ with zero average. A small (11 mV) systematic voltage offset in alternate rows associated with the alternating raster direction was also removed. Strong plateaus at integer modes in the leads are not seen, suggesting that considerable mode mixing occurs as the leads enter the dot. No changes in the statistics of $\delta g(V_g, B)$ are seen along the shape-distortion (V_g) direction.

A dominant feature in the conductance fluctuation landscape appears around $B = 0$ [Fig. 1(a)], associated with weak localization [5,6,22], or, equivalently, with the breaking of time-reversal symmetry by a magnetic field. As seen in Fig. 1, the average conductance is reduced and the variance of conductance fluctuations is increased in the vicinity of $B = 0$. Figure 1(b) quantifies the effect of weak localization on the average conductance $\langle g(B) \rangle$, where $\langle \cdot \rangle$ indicates an average over shape space, i.e., over V_g at fixed magnetic field. The B dependence of the shape-averaged conductance near $B = 0$ is in good agreement with the predicted Lorentzian line shape [22,23],

$$\langle g(B) \rangle = \langle g \rangle - \frac{\delta \langle g \rangle_{\mathrm{WL}}}{1 + (2B/\alpha' \phi_0)^2}, \qquad (1)$$

where $\langle g \rangle$ is the average conductance without weak localization, $\delta \langle g \rangle_{\mathrm{WL}}$ is the weak localization correction, α' the characteristic inverse area accumulated by coherent electrons traversing the dot, and ϕ_0 is the quantum of magnetic flux. A fit by Eq. (1) over the range $|B| < 0.8$ mT gives $\langle g \rangle = 1.93$, $\delta \langle g \rangle_{\mathrm{WL}} = 0.31$, and $\alpha' = 0.14 \pm 0.01$ μm^{-2}. We note that a characteristic "overshoot" in the vicinity of $|B| = 1.5$ mT causes this fit to slightly [(10–20)%] overestimate the value $\delta \langle g \rangle_{\mathrm{WL}}$. The prime on α' refers to the method used to determine its value; below, we will find a characteristic inverse area α from the power spectrum of magnetoconductance fluctuations, similar to the method used in Ref. [5], and find that the two values are in good agreement. This agreement is important given the expected absence of a thermal smearing term in α'. Our value for $\delta \langle g \rangle_{\mathrm{WL}}$ is smaller than the value 0.40 predicted by random matrix calculations [11,12] for two channels per lead, but is brought into agreement [15] by adding 6–8 channels to the random matrix theory to account for a finite phase breaking rate γ_φ. This number of phase breaking channels $N_\varphi \equiv (m^* A/\hbar)\gamma_\varphi$ [24] is determined independently based on the dependence of α on $\langle g \rangle$ [25].

We also observe an increase in the variance var$[g(B)]$ of shape-induced fluctuations as we move toward $B = 0$ with a similar characteristic field scale as the decrease in average conductance, as shown in Fig. 1(c). Lacking any rigorous theory, we assume a Lorentzian-squared form for the variance [26]

$$\mathrm{var}[g(B)] = \mathrm{var}(g) + \frac{\delta \mathrm{var}(g)}{[1 + (2B/\alpha'' \phi_0)^2]^2}, \qquad (2)$$

and find var$(g) = 0.015$, δvar$(g) = 0.019$, and $\alpha'' = 0.11 \pm 0.01$ μm^{-2}. Although Eq. (2) fits reasonably well over the range shown in Fig. 1(c), our data by no mean confirm this functional form. Overall, the variance is smaller by a factor of ~ 3 to 4 than predicted by random matrix calculations that do not include phase breaking [11,12], but appear consistent with theory once phase breaking channels and thermal averaging are included [15]. The added complication of thermal averaging can be circumvented by investigating the *ratio* of the zero-field variance to the finite-field variance [$= 1 + \delta$var$(g)/$var(g)]. In our experiment, this ratio is found to be 2.2 which agrees with random matrix calculations once the (independently determined) 6–8 channels of phase breaking are added [15]. Without phase breaking, the ratio is predicted to be 1.54 [12].

Figure 2 shows the continuous change in the distribution of conductance fluctuations across the transition from time-reversal symmetry to broken time-reversal symmetry. These figures show that all distributions appear reasonably well described by Gaussians, without any strong asymmetries. Again, this is in contrast to the results random matrix theory for two modes per lead [12,17], the difference being attributable to phase breaking [14,15].

Turning our attention to a new statistic, Fig. 3(b) shows the contour lines of the fluctuation landscape away from $B = 0$ [Fig. 3(a)]. The solid lines are contours near the average conductance, $\delta g(V_g, B) \sim 0$. These lines appear to percolate through the landscape, that is, one can follow a single line over a large part of the landscape. By

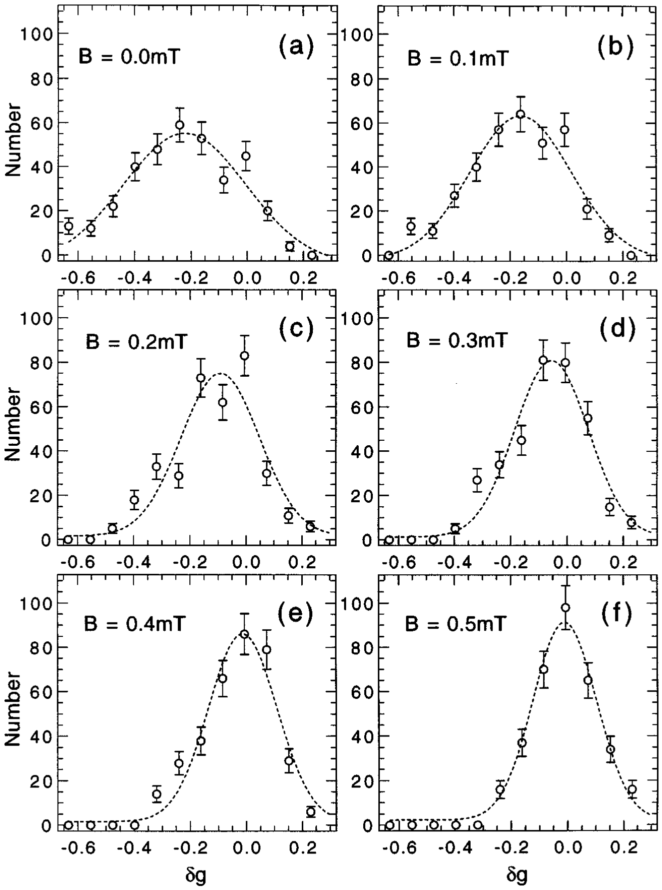

FIG. 2. (a)–(f) Evolution of the distribution of conductance fluctuations $\delta g(B)$ (in units of e^2/h) as time-reversal symmetry is broken. Distributions are histograms of shape-distortion conductance fluctuation data at each field (vertical scale is histogram bin count). The changes in mean and variance are expected from Figs. 1(b) and 1(c). The dashed lines are Gaussian fits.

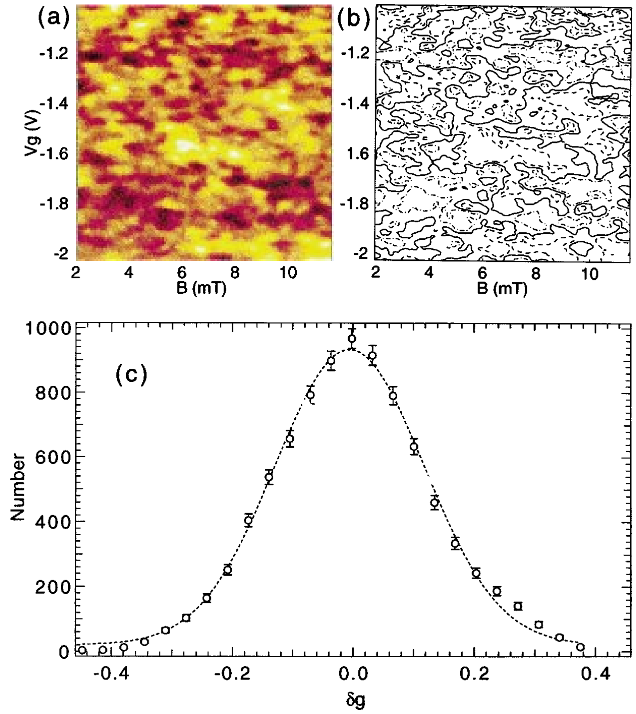

FIG. 3. (a) Color map of conductance fluctuations $\delta g(V_g, B)$ (in units of e^2/h) away from $B = 0$. (b) Contour map of (a). Solid curves are percolating contours near $\delta g(V_g, B) \sim 0$; dashed and dotted curves are at $\delta g(V_g, B) = +0.15$. (c) Distribution of conductance fluctuations $\delta g(V_g, B)$, found by constructing a histogram of the entire landscape of (a), is well described by a Gaussian (dashed curve).

contrast, the dashed and dotted lines are contours away from the average $\delta g(V_g, B) = \pm 0.15$, and typically enclose small regions of the landscape. The statistical properties of conductance contours depend on the fluctuation statistics, a connection well investigated within percolation theory [27]. Fluctuation contour lines not only provide a new probe of non-Gaussian statistics but also allow an estimate of the range of controllability of a mesoscopic device, for instance, in using shape distortion for feedback control of conductance in the presence of a changing external magnetic field. Figure 3(c) shows the distribution of conductance fluctuations from the entire surface. It is very well described by a Guassian, the expected result for a large number of channels [12,14,15].

Finally, we investigate correlations in the conductance fluctuation landscape by computing the power spectrum along both the shape-distortion and magnetic field directions. Each spectrum (Fig. 4) was estimated by averaging individual power spectra from uncorrelated horizontal or vertical strips of the landscape. These individual spectra were 64- or 128-point fast Fourier transforms averaged over half-overlapping windows along the strip. Eighteen strips were averaged for the magnetic field spectrum, and ten for the shape spectrum. A fit to the magnetic field spectrum S_B was made using the form predicted by semiclassical theory [8],

$$S_B(f_B) = S_B(0)\,(1 + 2\pi\alpha\phi_0 f_B)e^{-2\pi\alpha\phi_0 f_B}, \qquad (3)$$

where f_B is the magnetic frequency in cycles/T, and, as above, α is the characteristic inverse area of semiclassical trajectories. The fit was made over the range $500 < f_B < 2250$ cycles/T, yielding $\alpha = 0.14 \pm 0.01\ \mu\mathrm{m}^{-2}$, in agreement with the value α' derived from a fit to the weak localization conductance dip. This is an important agreement, as the role of thermal smearing in determining α remains controversial, whereas α' is not expected to be sensitive to thermal smearing.

A fit of the shape-distortion power spectrum S_v by an exponential form $S_V(f_V) = S_V(0)e^{-2\pi\kappa f_V}$ was performed over the range $5 < f_V < 45$ cycles/V, giving $\kappa = 29$ mV. An exponential form for the power spectrum, corresponding to a Lorentzian autocorrelation, is presumably appropriate when shape distortion alters the area of the device and so is comparable to a changing of the Fermi energy [28]. This form fits the data very well and gives a useful value for the characteristic voltage required to induce shape fluctuations in terms of the parameter κ. If this value $\kappa = 29$ mV is used to estimate a change in

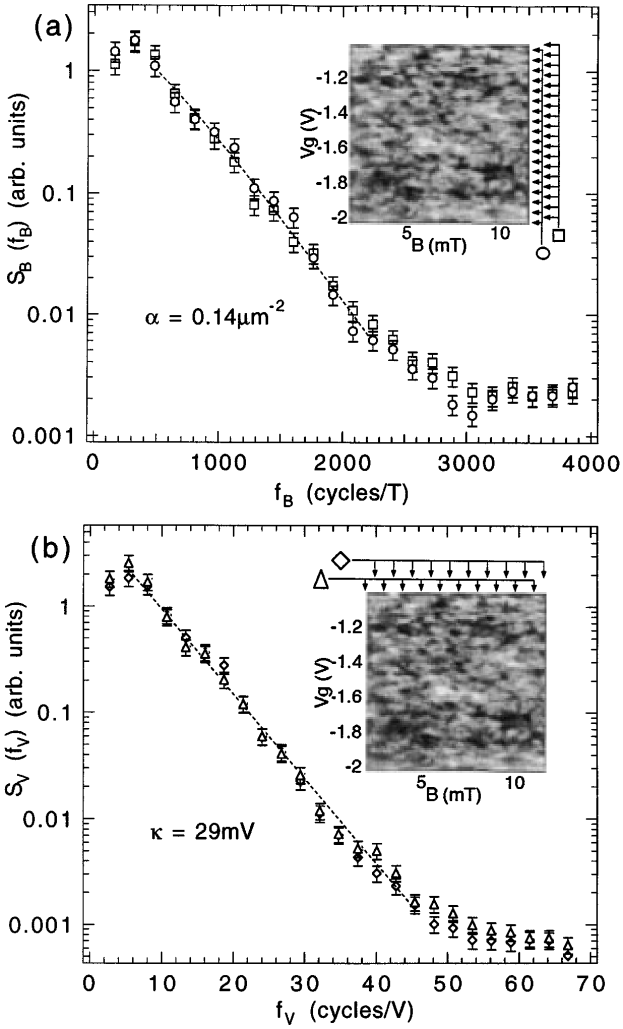

FIG. 4. (a) Shape-averaged power spectral density in magnetic field $S_B(f_B)$ away from $B = 0$, with arbitrary units. The dashed line is a fit of the circles to Eq. (3). The squares are averaged over a different region and shown for comparison. Inset: the uncorrelated horizontal strips of data over which the circles and squares were averaged. (b) Field-averaged ($B > 0$) power spectral density in shape (V_g), $S_V(f_V)$. The dashed line is a fit of the triangles to the exponential $S_V(f_V) = S_V(0)e^{-2\pi\kappa f_V}$. The diamonds are averaged over a different region for comparison. Inset: the uncorrelated vertical strips of data over which the triangles and diamonds were averaged.

the depletion width near the gate [21], the result is on the order of one-tenth the Fermi wavelength of the electrons.

In summary, we have investigated shape-distortion–induced conductance fluctuations in a quantum dot. Fluctuations are Gaussian distributed with continuous changes in mean and variance as time-reversal symmetry is broken. Including phase breaking in the theory is necessary for quantitative agreement with experimental results. Shape-distortion fluctuations appear well described by an exponential power spectrum.

We thank H. Baranger, H. Bruus, K. Efetov, and V. Falko for valuable discussions. This work was initiated with support from the Center for Materials Research at Stanford University under the NSF-MRL and partially supported by the ONR-YIP (Grant No. N00014-94-1-0622), and supported at UCSB by the AFOSR (Grant No. AFOSR-91-0214) and by QUEST, an NSF Science and Technology Center.

[1] B. L. Altshuler and B. I. Shklovskii, Sov. Phys. JETP **64**, 127 (1986).
[2] R. A. Jalabert, H. U. Baranger, and A. D. Stone, Phys. Rev. Lett. **65**, 2442 (1990).
[3] E. Doron, U. Smilansky, and A. Frenkel, Physica (Amsterdam) **50D**, 367 (1991).
[4] A. D. Stone, P. A. Mello, K. A. Muttalib, and J. Pichard, in *Mesoscopic Phemomena in Solids*, edited by B. L. Altshuler, P. A. Lee, and R. A. Webb (Elsevier, Amsterdam, 1991).
[5] C. M. Marcus *et al.*, Phys. Rev. Lett. **69**, 506 (1992).
[6] M. W. Keller, O. Millo, A. Mittal, and D. E. Prober, Surf. Sci. **305**, 501 (1994).
[7] C. W. J. Beenakker, Phys. Rev. Lett. **70**, 1155 (1993).
[8] H. A. Weidenmüller, Nucl. Phys. **A518**, 1 (1990).
[9] A. M. Chang, H. U. Baranger, L. N. Pfeiffer, and K. W. West, Phys. Rev. Lett. **73**, 2111 (1994).
[10] V. N. Prigodin, K. B. Efetov, and S. Iida, Phys. Rev. Lett. **71**, 1230 (1993).
[11] R. A. Jalabert, J.-L. Pichard, and C. W. J. Beenakker, Europhys. Lett. **27**, 255 (1994).
[12] H. U. Baranger and P. A. Mello, Phys. Rev. Lett. **73**, 142 (1994).
[13] U. Sivan *et al.*, Europhys. Lett. **25**, 605 (1994).
[14] P. W. Brouwer and C. W. J. Beenakker, Phys Rev. B **51**, 7739 (1995).
[15] H. U. Baranger and P. A. Mello, Phys Rev. B **51**, 4703 (1995).
[16] R. Schuster *et al.*, Phys. Rev. B **49**, 8510 (1994).
[17] H. Bruus and A. D. Stone, Phys. Rev. B **50**, 18 275 (1994).
[18] W. A. Lin, J. B. Delos, and R. V. Jensen, Chaos **3**, 655 (1993).
[19] M. J. Berry *et al.*, Surf. Sci. **305**, 495 (1994).
[20] L. P. Kouwenhoven *et al.*, Phys. Rev. B **40**, 8083 (1989).
[21] D. B. Chklovskii, B. I. Shklovskii, and L. I. Glazman, Phys. Rev. B **46**, 4026 (1992).
[22] H. U. Baranger, R. A. Jalabert, and A. D. Stone, Phys. Rev. Lett. **70**, 3876 (1993).
[23] Z. Pluhar *et al.*, Phys. Rev. Lett. **73**, 2115 (1994).
[24] C. M. Marcus, R. M. Westervelt, P. F. Hopkins, and A. C. Gossard, Phys. Rev. B **48**, 2460 (1993).
[25] R. M. Clarke *et al.*, "Temperature Dependence of Phase Breaking in Ballistic Quantum Dots" (to be published).
[26] K. B. Efetov (private communication).
[27] M. B. Isichenko, Rev. Mod. Phys. **64**, 961 (1992).
[28] V. Falko (private communication).